Integrating metabolic scaling and coexistence theories

Serguei Saavedra[1,2*], José Ignacio Arroyo[2], Jie Deng[1,3],
Pablo A. Marquet[2,4,5,6], Christopher P. Kempes[2]

[1]Department of Civil and Environmental Engineering, MIT,
77 Massachusetts Av., 02139 Cambridge, MA, USA

[2]Santa Fe Institute,
Santa Fe, NM 87501, USA

[3]Sir William Dunn School of Pathology, University of Oxford,
S Parks Rd, Oxford OX1 3RE, UK

[4]Department of Ecology & Evolutionary Biology, Princeton University,
Princeton, NJ 08544, USA

[5]Área de Biología Integrativa, Facultad de Ciencias Biológicas,
Pontificia Universidad Católica de Chile,
Santiago, 8331150, Chile

[6]Centro de Modelamiento Matemático,
Universidad de Chile, International Research Laboratory 2807, CNRS,
Santiago 8370456, Chile

[*]To whom correspondence should be addressed.
E-mail: sersaa@mit.edu

Keywords: feasibility | competition | coexistence | scaling | interactions | body size

Open Research: The code supporting the results is archived on Github:
`https://github.com/MITEcology/Scaling_Coexistence`. Upon acceptance, the code will be provided via Zenodo.

1

Abstract

Metabolic scaling theory has been pivotal in formalizing the expected energy expenditures across populations as a function of body size. Coexistence theory has provided a mathematization of the environmental conditions compatible with multispecies coexistence. Yet, it has been challenging to explain how observed community-wide patterns, such as the inverse relationship between population abundance density and body size, can be unified under both theories. Here, we provide the foundation for a tractable, scalable, and extendable framework to study the coexistence of resource-mediated competing populations as a function of their body size. For a given thermal domain and response, this integration reveals that the metabolically predicted 1/4 power dependence of carrying capacity of biomass density on body size can be understood as the average distribution of carrying capacities across feasible environmental conditions, especially for large communities. In line with empirical observations, our integration predicts that such average distribution leads to communities in which population biomass densities at equilibrium are independent from body size, and consequently, population abundance densities are inversely related to body size. This integration opens new opportunities to increase our understanding of how metabolic scaling relationships at the population level can shape processes at the community level under changing environments.

Metabolic scaling theory

Metabolism is the sum of the total biochemical reactions governing the flow of energy in an individual (Kleiber, 1932). Therefore, knowing how and why metabolism changes across individuals has become central in our understanding of the energy requirements driving the sustainability of different forms of life on Earth (Arroyo et al., 2022, Kempes et al., 2011, Maurer, 1996, Shestopaloff, 2024). In this line, metabolic scaling theory (Brown et al., 2004) has been instrumental in investigating whether the rate of energy expenditure in an individual scales with its body size (body mass) and temperature. The size and temperature dependence is expected as the result of the fractal-like design of the resource supply system and the kinetics of the metabolic reactions (Gillooly et al., 2001, West et al., 1997). These dependencies are described by simple equations. On the one hand, the size dependence is typically allometric (not proportional) power-law relationships of the form $y = a \cdot x^{\beta}$, where a is the constant of proportionality (normalization constant), and the sign and magnitude of the exponent (power) β phenomenologically represent the physico-chemical constraints operating at the individual level (Gillooly et al., 2001, 2002, West et al., 1997). On the other hand, the temperature response ($f(T)$) can be either exponential or unimodal (Arroyo et al., 2022, Dell et al., 2011, Gillooly et al., 2001, 2002, West et al., 1997).

Put together, it has been shown (Gillooly et al., 2001, 2002, West et al., 1997) that the metabolic rate (b_i) of an individual i is expected to scale with its body size (m_i) under a given temperature (T) as

$$b_i = b_0 \cdot f(T) \cdot m_i^{3/4} \tag{1}$$

(dimensions $[\text{mass}] \cdot [\text{time}]^{-1}$), where b_0 is a taxon-specific normalization constant (dimensions $[\text{mass}]^{1/4}[\text{time}]^{-1}$), and $f(T)$ is a generic thermal response (dimensionless). Eq. 1 reveals that larger individuals are expected to be characterized by higher energy requirements per unit of time. These requirements, however, are expected to decrease non-linearly per unit of mass as $b_i \cdot m_i^{-1} = b_0 \cdot f(T) \cdot m_i^{-1/4}$ (known as mass-specific metabolism, dimension $[\text{time}]^{-1}$), revealing the economies of body plans (Arroyo et al., 2022, Savage et al., 2004).

In community ecology (Vellend, 2016), populations (rather than individuals) are typically the basic units of living matter organization (Odum and Barrett, 2005, Vellend, 2016). Assuming a fixed growth rate of a population i under a constant environment, and that a stable age and size distribution have been reached, the average value of mass per individual (M_i) becomes time independent and the average metabolic rate (Eq. 1) of population i can be written as

3

$B_i = B_0 \cdot M_i^{3/4}$ (dimensions [mass]·[time]$^{-1}$) (Savage et al., 2004), where B_0 is a now an effective parameter for a given temperature and thermal response (dimension [mass]$^{1/4}$·[time]$^{-1}$). These metabolic scaling relationships have been confirmed by multiple empirical data across different taxa (Belgrano et al., 2002, Bernhardt et al., 2018, Damuth, 1987). However, the specific parameter values characterizing the metabolic dependence on temperature and size can vary as a function of the species and taxonomic group, respectively (Arroyo et al., 2022, Dell et al., 2011, Gillooly et al., 2001). For instance, it has been shown that for metazoans, protists, and prokaryotes, the scaling dependence of metabolic rate on body size ranges from sub-linear, linear, to super-linear, respectively (DeLong et al., 2010).

Similarly, it can then be predicted (Gillooly et al., 2002, Savage et al., 2004) that the maximum generation time (or lifespan) of an individual from population i becomes proportional to the scaling relationship $G_i \propto M_i^{\frac{1}{4}}$ (dimension [time]). Thus, the reciprocal of maximum generation time (i.e., mortality rate) is expected to be proportionally related to the maximum growth rate of an individual in population i and can be written as

$$\frac{1}{G_i} \propto r_i = r_0 \cdot M_i^{-1/4} \tag{2}$$

(dimension [time]$^{-1}$), where r_0 is an effective parameter for a given temperature and thermal response (dimension [mass]$^{1/4}$ · [time]$^{-1}$). These relationships have been used to show how the metabolic processes at the level of individuals can affect the metabolic and ecological processes at the level of populations (Savage et al., 2004).

Moreover, assuming that individuals from a population with different body sizes capture, on average, the same amount of resources or energy in their environment (i.e., the energetic equivalence rule (Damuth, 1987)), it has been shown (Savage et al., 2004) that it is possible to derive the mass and temperature dependence of a population's carrying capacity of biomass density. This is the predicted, maximum, biomass density of a population in isolation that can be sustained and can be written as

$$K_i = K_0 \cdot M_i^{-3/4} \cdot M_i = K_0 \cdot M_i^{1/4} \tag{3}$$

(dimensions [mass]·[area]$^{-1}$), where K_0 is an effective parameter (dimensions [mass]$^{3/4}$·[area]$^{-1}$). That is, under a given temperature and thermal response, the maximum biomass of a population in isolation per unit area is expected to increase with size. Note that this is different from the carrying capacity of abundance density $K_i^a = K_i/M_i$ (dimensions [individuals]·[area]$^{-1}$), which

4

78 is expected to decrease with body size as $K_i^a \propto M_i^{-3/4}$ (Damuth, 1987).

79 Understanding how these different scaling relationships at the individual (or population level)
80 are linked to ecological processes at the community level (the collection of different interacting
81 populations in a given place and time) is challenging, and while there has been significant
82 empirical and theoretical work using metabolic scaling theory at the community level (Basset
83 and Angelis, 2007, Brose et al., 2006, Marquet et al., 2004, 1990, 2005, Tabi et al., 2023, Vasseur
84 and McCann, 2005, Yeakel et al., 2018, Yodzis and Innes, 1992), several important challenges for
85 theoretical integration and simplification still remain open. A clear example is the relationship
86 between the distribution of body sizes and the coexistence of multiple populations, which has
87 been typically studied for a specific set of model parameters (Brose et al., 2006, Yodzis and
88 Innes, 1992). As a consequence, it is unclear the extent to which both the coexistence of
89 multiple populations as well as their biomass densities depend on the distribution of body sizes
90 (Bideault et al., 2021, Brose et al., 2006, DeLong et al., 2010, Hatton et al., 2019, Savage et al.,
91 2004). Similarly, there is still theoretical work to be done in order to increase our understanding
92 of how metabolic scaling relationships at the individual or population levels affect coexistence
93 processes at the community level (Arim et al., 2007, Basset and Angelis, 2007, Hatton et al.,
94 2024, Savage et al., 2004).

Coexistence theory

96 In general, coexistence theory in ecology (Chesson, 2000, MacArthur and Levins, 1967, Saave-
97 dra et al., 2017, Vandermeer, 1970) aims to investigate the possibility that a community $\mathcal{S}(\mathbf{A})$,
98 formed by $|\mathcal{S}|$ populations and characterized by an interaction matrix ($\mathbf{A}$), can persist under
99 different environmental contexts. Although not exclusively, this analysis has been mainly per-
100 formed under generalized Lotka-Volterra dynamics (Case, 2000), which in line with metabolic
101 scaling theory (Brown et al., 2004), can be derived from thermodynamics principles, from prin-
102 ciples of conservation of mass and energy, and from chemical kinetics in large populations (Lo-
103 gofet, 1993, Lotka, 1920, Michaelian, 2005, Täuber, 2011). In particular, in the Lotka-Volterra
104 competition model (Arditi et al., 2021, Medeiros et al., 2021a), the per capita growth rate of a
105 population's biomass density can be written as

$$\frac{\dot{N}_i}{N_i} = \frac{r_i}{K_i}(K_i - \sum_j a_{ij} \cdot N_j), \forall i \in \mathcal{S}(\mathbf{A}), \tag{4}$$

5

106 (dimension $[\text{time}]^{-1}$), where N_i is the population biomass density (dimensions $[\text{mass}]\cdot[\text{area}]^{-1}$)

107 and $\dot{N}_i$ is the time derivative (dimensions $[\text{mass}]\cdot[\text{area}]^{-1}\cdot[\text{time}]^{-1}$). Here, $r_i > 0$ is the max-

108 imum intrinsic growth rate (dimension $[\text{time}]^{-1}$), $K_i > 0$ is the carrying capacity of biomass

109 density (dimensions $[\text{mass}]\cdot[\text{area}]^{-1}$). Then, $\mathbf{A} = (a_{ij}) \geq 0 \in \mathbb{R}^{|\mathcal{S}|\times|\mathcal{S}|}$ is the per capita, time-

110 independent, area-independent, competitive effect (dimensions $[\text{mass}_i]\cdot[\text{mass}_j]^{-1}$) of a popula-

111 tion j on an individual of population i. Note that

$$a_{ij} = \frac{\hat{a}_{ij}}{\hat{a}_{ii}}, \tag{5}$$

112 where $\hat{a}_{ij}$ and $\hat{a}_{ii}$ are the competitive effects across unit area (dimensions $[\text{time}]^{-1}\cdot[\text{mass}_j]^{-1}\cdot[\text{area}]$)

113 and self-regulation (dimensions $[\text{time}]^{-1}\cdot[\text{mass}_i]^{-1}[\text{area}]$), respectively. It follows that $a_{ii} = 1$

114 per definition. In other words, a_{ij} specifies the time-independent, area-independent rate of

115 biomass converted from a population i to a population j (or resources used by j instead of i)

116 (Logofet, 1993). Then, the carrying capacity of biomass density of a population i under a given

117 environment can be expressed as a function of its intrinsic growth rate and self-regulation as

$$K_i = \frac{r_i}{\hat{a}_{ii}}. \tag{6}$$

118 The necessary condition for persistence under Lotka-Volterra equilibrium dynamics (i.e., $\dot{N}_i =$

119 0) becomes the existence of positive solutions in population biomass densities (Hofbauer and

120 Sigmund, 1998). This necessary condition is known as *feasibility* and takes the form of a linear

121 equation in matrix notation (Saavedra, 2024, Vandermeer, 1970))

$$\boldsymbol{N}^* = \mathbf{A}^{-1}\boldsymbol{K}^* > 0, \tag{7}$$

122 where the vector $\boldsymbol{N}^*$ represents the distribution of biomass densities at equilibrium, $\mathbf{A}^{-1}$ corre-

123 sponds to the inverse of the interaction matrix, and the vector $\boldsymbol{K}^*$ is the distribution of carrying

124 capacities of biomass densities compatible with the feasibility of community $\mathcal{S}(\mathbf{A})$. Notice that

125 it is possible to multiply the vector $\boldsymbol{K}^*$ by any positive scalar ($\lambda > 0$) and the feasibility con-

126 dition (i.e., $\boldsymbol{N}^* = \mathbf{A}^{-1}\boldsymbol{K}^*\lambda > 0$) does not change. This is true because the relationship among

127 carrying capacities of biomass densities within the community does not change (i.e., all values

128 are either increased or decreased proportionally). Of course, if λ approaches zero, the loss of

129 feasibility can happen due to stochasticity (Hofbauer and Sigmund, 1998). This implies that

130 given an interaction matrix, the feasibility of a community is determined by the direction rather

131 than the magnitude of the vector (Saavedra et al., 2017). In other words, feasibility depends

on the relationship (or distribution) among carrying capacities of biomass densities within the community.

Importantly, there can be more than one compatible vector $\boldsymbol{K}^*$. This possible set of vectors is known as the feasibility domain (D_F) (Logofet, 1993, Saavedra et al., 2017). Formally, rearranging Eq. 7 and solving for $\boldsymbol{K}^*$, this feasibility domain can be expressed as

$$D_F(\mathcal{S}(\mathbf{A})) = \left\{ \boldsymbol{K}^* = \sum_{j \in \mathcal{S}} N_j^* \mathbf{a}_j : \mathbf{A} = [\mathbf{a}_1 \ \mathbf{a}_2 \ \cdots \ \mathbf{a}_{|\mathcal{S}|}], N_j^* \in \mathbb{R}_{>0} \right\} \in \mathbb{R}^{|\mathcal{S}|}, \tag{8}$$

where $\mathbf{a}_j$ is the jth column vector of the interaction matrix $\mathbf{A}$ (Logofet, 1993, Song and Saavedra, 2018). Each column j represents the time-independent, area-independent, competitive effect of population j on all other populations (including itself). The feasibility domain specifies all the possible distributions (vector directions) of $\boldsymbol{K}$ (Eq. 6) that are compatible with the interaction matrix $\mathbf{A}$ as written in Eq. (7). Geometrically, the feasibility domain is the convex hull of the $|\mathcal{S}|$ spanning vectors in $|\mathcal{S}|$-dimensional space (Fig. 1) (Deng et al., 2023, 2022, Song et al., 2018b). Overall, the interaction matrix $\mathbf{A}$ determines the range of the feasibility domain. The stronger the mean competition in a community ($\langle a_{ij} \rangle$), the smaller the range of the feasibility domain (Saavedra et al., 2017).

For a given community characterized by a particular interaction matrix, the location of a given vector $\boldsymbol{K}^*$ inside the feasibility domain provides information about a given set of environmental conditions compatible with the feasibility of such community (i.e., $\boldsymbol{N}^* > 0$). Formally, the geometric centroid of the feasibility domain (Fig. 1) can be understood as the average distribution of carrying capacities of biomass densities across all feasible environments. This statement makes the assumption that the elements of the vector of carrying capacities of biomass densities are independent from each other and free to vary due to external factors other than temperature, such as long-term changes in species habitats. Formally, the geometric centroid can be calculated as (Medeiros et al., 2021b, Song and Saavedra, 2018, Tabi et al., 2020)

$$\boldsymbol{K_c}(\mathbf{A}) = |\mathcal{S}|^{-1} \boldsymbol{a}_1 + \cdots + |\mathcal{S}|^{-1} \boldsymbol{a}_n. \tag{9}$$

Moreover, by mathematical definition, the centroid $\boldsymbol{K_c}(\mathbf{A})$ yields the solution (Rohr et al., 2016)

$$\boldsymbol{N}^* = \mathbf{A}^{-1} \boldsymbol{K_c^*} = (h, h, \ldots, h) \in \mathcal{R}^{|\mathcal{S}|}, \tag{10}$$

where $h > 0$ is a positive constant. That is, while the elements of the vector of carrying capacities

7

of biomass densities defining the centroid of the feasibility domain can be different from each other, the populations' biomass densities become the same at equilibrium and independent from body size.

Integrating theories

The link between metabolic scaling and population dynamics has been performed under different frameworks, each answering specific ecological questions (Basset and Angelis, 2007, Brose et al., 2006, Campillay-Llanos et al., 2022, Harte et al., 2008, Parain et al., 2019, Vasseur and McCann, 2005, Yeakel et al., 2018, Yodzis and Innes, 1992, Zaoli et al., 2017). Here, we provide a tractable, scalable, and extendable framework to study the effect of body size on the feasibility of resource-mediated competing populations. Specifically, we aim to investigate the possibility that a community of competing populations characterized by a given distribution of body sizes can coexist under different environmental contexts. To this end, our framework is based on Lotka-Volterra competition dynamics (Vandermeer and Goldberg, 2013).

Under resource-mediated competition models, it is assumed that the dynamics of resources are faster than that of consumers. While this is a strong assumption, classic and recent work has shown promising approximations to empirical competition dynamics (MacArthur and Levins, 1967, Medeiros et al., 2021a, Parain et al., 2019, Song et al., 2018a). Following this premise, time-independent, area-independent, competitive interactions (a_{ij}) can be written as a function of the average consumption rates of consumers (Fig. 1, see Appendix S1 for details):

$$a_{ij} = a'_0 \cdot \left(\frac{C_j}{C_i} \right), \tag{11}$$

where C_i corresponds to the time-independent, average consumption rate for a population i across unit area (dimensions $[\text{mass}_i]^{-1} \cdot [\text{area}]$), and a'_0 is an *effective* parameter representing the overall effect of intrinsic properties (dimensionless), such as consumers' conversion rates (Parain et al., 2019). Similarly, following single population models (Deng et al., 2024), the time-independent, average consumption rate of consumer i can be expressed as a function of its demographics (Fig. 1, see Appendix S1 for details):

$$C_i = \frac{1}{K_i \left(1 + d_i / r_i \right)}, \tag{12}$$

where d_i denotes the mortality rate (dimension $[\text{time}]^{-1}$), and K_i and r_i represent again the carrying capacities of biomass densities and maximum growth rate of consumer i, respectively.

Then, we can integrate metabolic scaling theory (Eqs. 2-3) and coexistence theory (Eq. 12) to write

$$C_i = C_0 \cdot M_i^{3/4} \cdot M_i^{-1} = C_0 \cdot M_i^{-1/4}, \tag{13}$$

where C_0 is a new effective parameter (dimensions $[\text{mass}]^{-3/4} \cdot [\text{area}]$). Note that studies have also found different scaling dependencies between consumption rate and body size (Pawar et al., 2012). As we will show below, these differences do not affect our conclusions. Thus, for a fixed temperature and thermal response, we can integrate Eqs. 11 and 13 as

$$a_{ij} = a_0 \cdot (M_j/M_i)^{-1/4}, \tag{14}$$

where a_0 is yet again a new effective parameter ($[\text{mass}_i]^{3/4} \cdot [\text{mass}_j]^{-3/4}$). In sum, for a given thermal domain and response, it is expected that the higher the average body size of population j relative to that of population i, the lower the time-independent, area-independent, competitive effect.

Next, we investigated the link between the feasibility of a community and the distribution of body sizes for a fixed temperature in metabolically-generated competition matrices $\mathbf{A}$. In particular, we systematically studied the scaling relationship β between the vector of carrying capacities of biomass densities and the vector of body sizes ($\boldsymbol{K} = \boldsymbol{K_0} \cdot \boldsymbol{M^\beta}$) that makes $\boldsymbol{K}$ close to the centroid of the feasibility domain ($\boldsymbol{K_c}(\mathbf{A})$). Recall that the centroid represents the average of carrying capacities of biomass densities across feasible environmental conditions, as expressed in Eq. 7.

Specifically, following Eq. 14, we generated an ensemble of 10^4 competition matrices $\mathbf{A}$ characterizing the time-independent, area-independent, competitive effects (a_{ij}) between 50 populations (larger dimensions yield similar conclusions, see Appendix S1). Each matrix was formed by drawing M_i values independently from a lognormal distribution $LN(0,2)$. These distributions can change without affecting the qualitative results. Following previous work (Bunin, 2017, Dougoud et al., 2018), we set the effective parameter of competitive effects to $a_0 = |\mathcal{S}|^{-1/2}$ for $i \neq j$, otherwise $a_0 = 1$. This assumption follows the rationale that empirical interactions tend to be weak, stabilizing communities (Gellner et al., 2023, McCann et al., 1998). The greater the value of a_0, the greater the overall competition, and the smaller the range of the feasibility domain. Then, for regular intervals between $\beta \in [-2, 2]$ (used as representative values), we calculated the average distance between $\boldsymbol{K_c}(\mathbf{A})$ and $\boldsymbol{K}$ as (Medeiros et al., 2021b, Saavedra

213 et al., 2017)

$$d(\mathbf{A}, \boldsymbol{K}) = \arccos(\boldsymbol{K} \cdot \boldsymbol{K_c}(\mathbf{A}) \cdot ||\boldsymbol{K}||^{-1} \cdot ||\boldsymbol{K_c}(\mathbf{A})||^{-1}) \in [0, 90]. \tag{15}$$

214 Note that the normalization constant K_0 of carrying capacities of biomass densities does not
215 affect this distance and can be omitted from the equation (Rohr et al., 2016).

216 Figure 2 reveals that the vector of carrying capacities of biomass densities described by the
217 scaling relationship $\boldsymbol{K} \propto \boldsymbol{M}^{\beta=\frac{1}{4}}$ gets close to the centroid of the feasibility domain of the
218 metabolically-generated competition matrices for a given thermal domain and response. For few
219 competing species (e.g., two), it will be exactly the centroid only for a particular value of a_0 (see
220 Appendix S1). This vector tends to get asymptotically closer to the centroid of the feasibility
221 domain the larger the community (see Appendix S1 for numerical analysis). This reveals that
222 the expected 1/4 power dependence of carrying capacities of biomass densities on body size can
223 be understood as the average distribution of carrying capacities across feasible environmental
224 conditions, especially for large communities. Furthermore, because the centroid represents the
225 condition under which all populations have the same biomass densities at equilibrium (Eq. 10),
226 dividing these biomass densities ($\boldsymbol{N^*}$) by the corresponding average body size $\boldsymbol{M}$, the number of
227 individuals per area ($\boldsymbol{I}$) become inversely related to body size ($\boldsymbol{I} \propto \boldsymbol{M}^{-1}$). This mathematical
228 fact is independent from the scaling exponent defining the dependency of consumption rate and
229 body size (Pawar et al., 2012). This implies that our framework is in agreement with empirical
230 observations showing that, at the community level (or over a much larger size range of life), a
231 population's abundance density scales inversely with body size (Hatton et al., 2019, Marquet
232 et al., 1990, Segura and Perera, 2023).

233 Concluding remarks

234 We have proposed an tractable, scalable, and extendable integration of metabolic scaling the-
235 ory (Brown et al., 2004) and coexistence theories (Chesson, 2000, MacArthur and Levins, 1967,
236 Saavedra et al., 2017, Vandermeer, 1970) in order to systematically link metabolic scaling rela-
237 tionships at the population level to community coexistence (Deng et al., 2021, 2022, Saavedra
238 et al., 2020). Our framework has been based on understanding how body-size constraints, op-
239 erating on competitive effects, modulate the parameter space of carrying capacities of biomass
240 densities compatible with multispecies coexistence. This integration has allowed us to show that
241 the metabolically predicted 1/4 power dependence of carrying capacities of biomass densities on
242 body size can be understood as the average distribution of biomass carrying capacities across

10

feasible environmental conditions, especially for large communities. Additionally, in line with empirical observations (Hatton et al., 2019), our integration conforms to the expectation that biomass densities at equilibrium are independent from body size, and consequently, to abundance densities at equilibrium that are inversely related to body size. Therefore, our framework can be used to link competitive effects to metabolism and, consequently, to body size, helping to capture important theoretical derivations and empirical observations (Hatton et al., 2019, Savage et al., 2004).

It is worth mentioning that our efforts to integrate metabolic scaling and coexistence theories have been simplified under a formalism that uses a set of relevant assumptions. In particular, we have focused on resource-mediated competition assuming that the dynamics of resources are faster than that of consumers. While there is a strong tradition on this type of competition systems, this does not take into account other type of much richer dynamics, such as as trophic interactions. However, previous efforts on these forms of dynamics (Parain et al., 2019, Vasseur and McCann, 2005) can be compatible with our framework (Saavedra et al., 2016). Similarly, we have exclusively focused on feasibility (the necessary condition for species coexistence under equilibrium dynamics) without systematically investigating dynamical stability (Song and Saavedra, 2018). For instance, future work can expand our work in order to investigate the role of life-history traits acting on interspecific effects in shaping both the feasibility and dynamical stability of communities. Additionally, while our results on the distance to the centroid of the feasibility domain are valid for a fixed thermal domain and response, feasibility itself can change as a function of temperature via changes in interspecific effects. Thus, for cases where the interest is to predict how a population or community will respond to temperature, it would be useful to use a model that accounts for the curvature of temperature responses (Arroyo et al., 2022, Dell et al., 2011). This alternative model can be adapted to our integration (by separating the role of temperature from the effective parameters) to explore temperature-related questions, such as how the variation in optimum temperatures of populations in a community would affect its feasibility or how global warming may alter communities. We believe the proposed integration can open up new opportunities to increase our understanding of how metabolic scaling relationships at the individual and population levels shape processes at the community level.

12

A Metabolic Scaling Theory

$r_i = r_0 M_i^{-1/4}$ (maximum growth rate)

$d_i = d_0 M_i^{-1/4}$ (mortality rate)

$K_i = K_0 M_i^{1/4}$ (carrying capacity of biomass density)

C Competition Theory

$a_{ij} = a_0' \dfrac{C_j}{C_i}$ (competitive interaction)

$C_i = \dfrac{1}{K_i\left(1 + \dfrac{d_i}{r_i}\right)}$ (consumption rate)

D Integration

For fixed temperature $C_i = C_0 M_i^{-1/4}$

$$a_{ij} = a_0 \left(\frac{M_j}{M_i}\right)^{-1/4}$$

B Coexistence Theory

- Carrying capacity of species 2 (K_2)
- Effect of species 2 on species 1, $\mathbf{a_2} = [a_{12}, a_{22}]$
- Ω Size of feasibility domain
- Centroid of feasibility domain $\mathbf{K_c} = |S|^{-1}(\mathbf{a_1} + \mathbf{a_2})$
- $\angle$ Distance between $\mathbf{K_c}$ and $\mathbf{K}$
- Realized carrying capacities $\lambda \mathbf{K} \propto \lambda \mathbf{M}^\beta; \lambda > 0$
- Effect of species 1 on species 2, $\mathbf{a_1} = [a_{11}, a_{21}]$
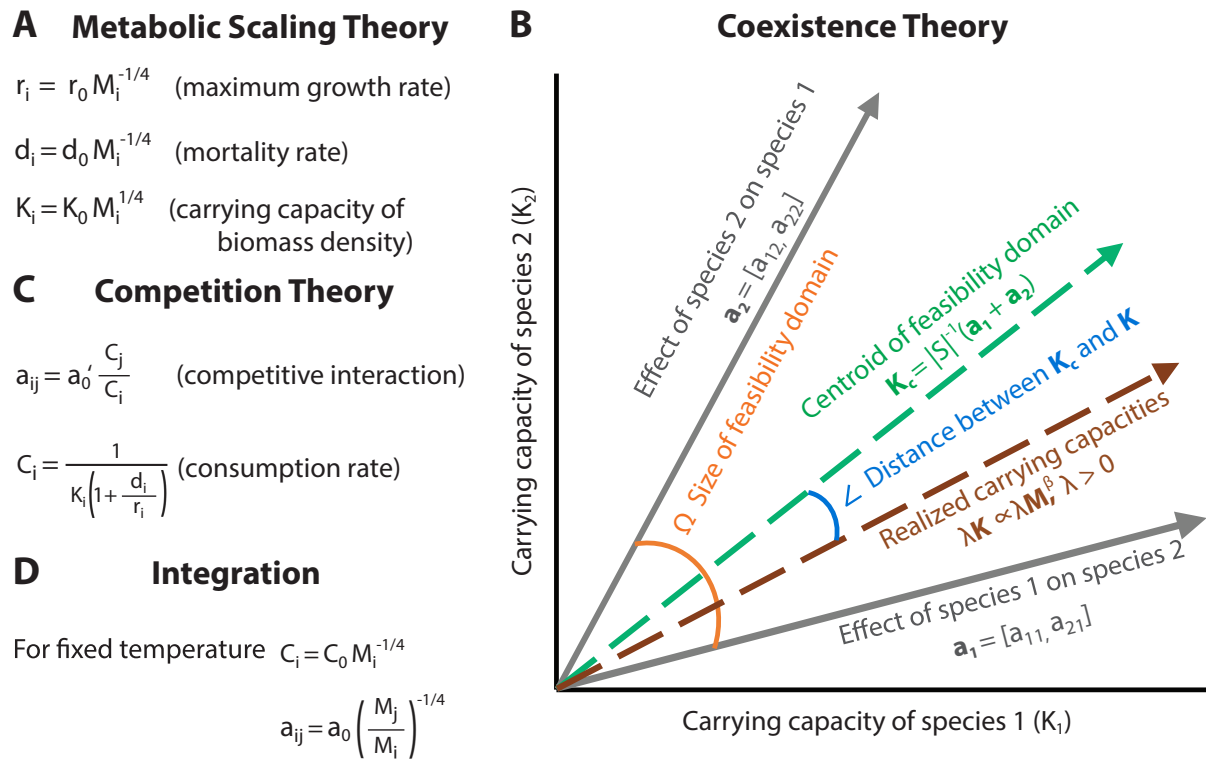- Carrying capacity of species 1 (K_1)

Figure 1: **A graphical integration of metabolic scaling and coexistence theories**. (**A**) Following metabolic scaling theory, for a given temperature and thermal response, maximum growth rate, mortality rate, and carrying capacities of biomass densities are predicted to scale as a function of body mass. (**B**) Following coexistence theory and under Lotka-Volterra competition dynamics (see main text), the feasibility (i.e., positive biomass densities at equilibrium) of a community will be defined by having the relationship (vector direction) among carrying capacities inside the domain constrained by species interactions. As an illustrative example, we show the parameter space (Cartesian coordinate system) of carrying capacities of biomass densities K_i of a community with $|S| = 2$ populations. The outer solid gray arrows correspond to the column vectors of the interaction matrix ($\mathbf{A} = [\mathbf{a_1}; \mathbf{a_2}]$). The angle (orange large curve) formed by the two column vectors corresponds to the feasibility domain $D_F(\mathcal{S}(\mathbf{A}))$ (Eq. 8). Inside the two column vectors, any direction of carrying capacities $\mathbf{K}$ is compatible with positive biomass densities at equilibrium (Eq. 7). In this sense, the direction (rather than the magnitude) defines the feasibility of a community. The centered green vector depicts the geometric centroid of the feasibility domain (Eq. 9, $\mathbf{K_c}$), representing the average distribution of carrying capacities of biomass densities across feasible environmental conditions for large communities. While the elements of $\boldsymbol{K_c}(\mathbf{A})$ can be different from each other, the centroid corresponds to the carrying capacities that provide the solution where all biomass densities are equal. (**C**) Following competition theory (see main text), we can define the time-independent, area-independent competitive effect (a_{ij}) of species j on i as a function of the average consumption rates, which can also be expressed as a function the maximum growth rate, mortality rate, and carrying capacity of biomass densities. (**D**) Integrating theories (see main text), for a fixed temperature, we can then express both the average consumption rates and the competitive effect as a power law function of body size.
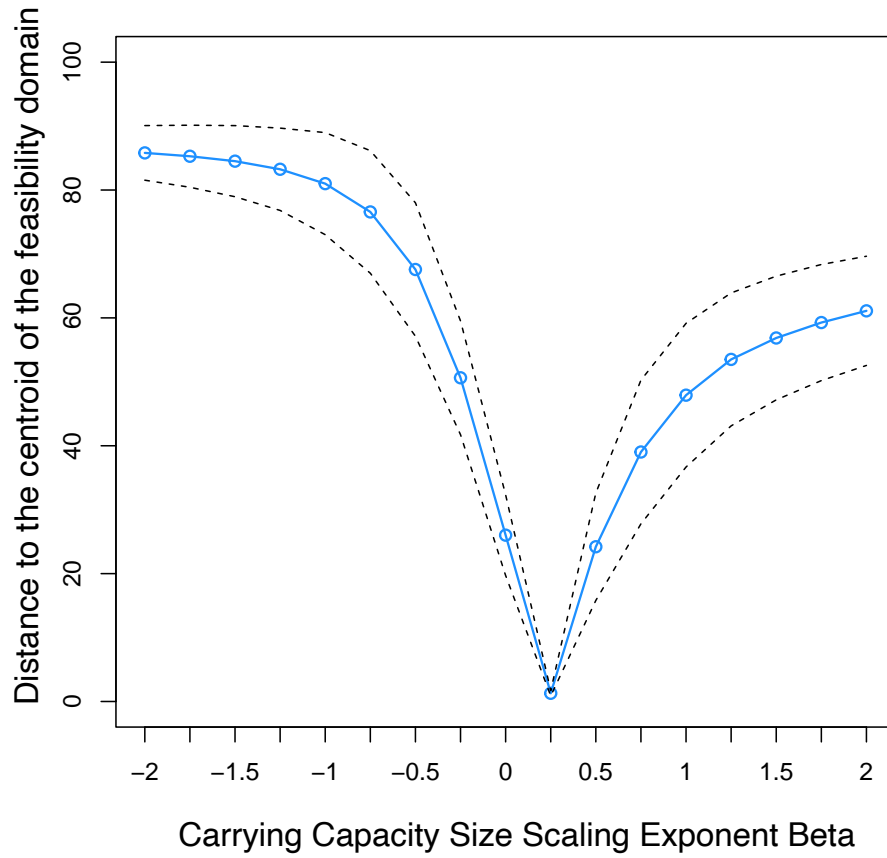
Figure 2: **Theoretical predictions**. For an ensemble of 10^6 communities with $|S = 50|$ populations, the blue solid line shows the average distance (Eq. 27, blue small curve in Figure 1) between the centroid of the feasibility domain $\mathbf{K_c}$ and the possible vectors of carrying capacities of biomass densities ($\boldsymbol{K} \propto \boldsymbol{M}^{\beta}$) as a function of the power exponent beta ($\beta \in [-2, 2]$) describing the dependence of carrying capacities on body size. The black dashed lines correspond to the average plus minus two standard deviations. For each community, the interaction matrix (Eq. 11) is defined by $\alpha = -1/4$ and $a_0 = |S|^{-1/2}$. The values of M_i are drawn independently from a lognormal distribution $LN(0, 2)$. For large communities, $\beta = 1/4$ tends to be the closest to the centroid (see Supplementary Information for more details).

References

Arditi, R., Tyutyunov, Y. V., Titova, L. I., Rohr, R. P., and Bersier, L. F. 2021. The dimensions and units of the population interaction coefficients. Frontiers Ecol. Evol. 9:775754.

Arim, M., Bozinovic, F., and Marquet, P. A. 2007. On the relationship between trophic position, body mass and temperature: reformulating the energy limitation hypothesis. Oikos 116:1524–1530.

Arroyo, J. I., Díez, B., Kempes, C. P., West, G. B., and Marquet, P. A. 2022. A general theory for temperature dependence in biology. PNAS 119:e2119872119.

Basset, A. and Angelis, D. L. 2007. Body size mediated coexistence of consumers competing for resources in space. Oikos 116:1363–1377.

Belgrano, A., Allen, A. P., Enquist, B. J., and Gillooly, J. F. 2002. Allometric scaling of maximum population density: a common rule for marine phytoplankton and terrestrial plants. Ecology Letters 5:611–613.

Bernhardt, J. R., Sunday, J. M., and O'Connor, M. I. 2018. Metabolic theory and the temperature-size rule explain the temperature dependence of population carrying capacity. The American Naturalist 192:687–697.

Bideault, A., Galiana, N., Zelnik, Y. R., Gravel, D., Loreau, M., Barbier, M., and Sentis, A. 2021. Thermal mismatches in biological rates determine trophic control and biomass distribution under warming. Global Change Biology 27:257–269.

Brose, U., Williams, R. J., and Martinez, N. D. 2006. Allometric scaling enhances stability in complex food webs. Ecology Letters 9:1228–1236.

Brown, J. H., Gillooly, J. F., Allen, A. P., M., V., and West, G. B. 2004. Toward a metabolic theory of ecology. Ecology 85:1771–1789.

Bunin, G. 2017. Ecological communities with Lotka-Volterra dynamics. Physical Review E 95:042414.

Campillay-Llanos, W., Córdova-Lepe, F. D., and Moreno-Gómez, F. N. 2022. Coexistence, energy, and trophic cascade in a three-level food chain integrating body sizes. Frontiers in Ecol. and Evol. 10:821176.

Case, T. J., 2000. An Illustrated Guide to Theoretical Ecology. Oxford Univ. Press, Oxford.

15

309 Chesson, P. 2000. Mechanisms of maintenance of species diversity. Annual review of Ecology
310 and Systematics 31:343–366.

311 Damuth, J. 1987. Interspecific allometry of population density in mammals and other animals:
312 the independence of body mass and population energy use. Biological Journal of the Linnaean
313 Society 31:193–246.

314 Dell, A. I., Pawar, S., and Savage, V. M. 2011. Systematic variation in the temperature
315 dependence of physiological and ecological traits. Proc. Natl. Acad. Sci. USA 108:10591–
316 10596.

317 DeLong, J. P., Okie, J. G., Moses, M. E., Sibly, R. M., and Brown, J. H. 2010. Shifts in
318 metabolic scaling, production, and efficiency across major evolutionary transitions of life.
319 Proceedings of the National Academy of Sciences 107:12941–12945.

320 Deng, J., Angulo, M. T., and Saavedra, S. 2021. Generalizing game-changing species across
321 microbial communities. ISME Communications 1:1–8.

322 Deng, J., Cordero, O. X., Fukami, T., Levin, S. A., Pringle, R. M., Solé, R., and Saavedra, S.
323 2024. The development of ecological systems along paths of least resistance. Current Biology
324 34:1–11.

325 Deng, J., Taylor, W., Levin, S. A., and Saavedra, S. 2023. On the limits to invasion prediction
326 using coexistence outcomes. J. of Theoretical Biology 577:111674.

327 Deng, J., Taylor, W., and Saavedra, S. 2022. Understanding the impact of third-party species
328 on pairwise coexistence. PLoS Comput. Biol. 18:e1010630.

329 Dougoud, M., Vinckenbosch, L., Rohr, R. P., Bersier, L. F., and Mazza, C. 2018. The feasibility
330 of equilibiria in large ecosystems: a primary but neglected concept in the complexity-stability
331 debate. PLOS Computational Biology 14:e1005988s.

332 Gellner, G., McCann, K., and Hastings, A. 2023. Stable diverse food webs become more
333 common when interactions are more biologically constrained. PNAS 120:e2212061120.

334 Gillooly, J. F., Brown, J. H., West, G. B., Savage, V. M., and Charnov, E. L. 2001. Effects of
335 size and temperature on metabolic rate. Science 293:2248–2251.

336 Gillooly, J. F., Charnov, E. L., West, G. B., Savage, V. M., and Brown, J. H. 2002. Effects of
337 size and temperature on developmental time. Nature 417:70–73.

Harte, J., Zillio, T., Conlisk, E., and Smith, A. B. 2008. Maximum entropy and the state-variable approach to macroecology. Ecology 89:2700–2711.

Hatton, I. A., Dobson, A. P., Storch, D., and Loreau, M. 2019. Linking scaling laws across eukaryotes. PNAS 116:21616–21622.

Hatton, I. A., Mazzarisi, O., Altieri, A., and Smerlak, M. 2024. Diversity begets stability: Sublinear growth and competitive coexistence across ecosystems. Science 383:1196.

Hofbauer, J. and Sigmund, K., 1998. Evolutionary games and population dynamics. Cambridge University Press.

Kempes, C. P., Dutkiewicz, S., and Follows, M. J. 2011. Growth, metabolic partitioning, and the size of microorganisms. PNAS 109:495–500.

Kleiber, M. 1932. Body size and metabolism. Hilgardia 6:315–353.

Logofet, D. O., 1993. Matrices and Graphs: Stability Problems in Mathematical Ecology. CRC Press.

Lotka, A. J. 1920. Analytical note on certain rhythmic relations in organic systems. Proceedings of the National Academy of Sciences 6:410–415.

MacArthur, R. and Levins, R. 1967. The limiting similarity, convergence, and divergence of coexisting species. Am. Nat. 101:377–385.

Marquet, P. A., Labra, F. A., and Maurer, B. A. 2004. Metabolic ecology: linking individuals to ecosystems. Ecology 85:1794–1796.

Marquet, P. A., Navarrete, S. A., and Castilla, J. C. 1990. Scaling population density to body size in rocky intertidal communities. Science 250:1125–1127.

Marquet, P. A., Quiñones, R. A., Abades, S., Labra, F. A., Tognelli, M., Arim, M., and Rivadeneira, M. 2005. Scaling and power-laws in ecological systems. Journal of Experimental Biology 208:1749–1769.

Marshall, D. J., Cameron, H. E., and Loreau, M. 2023. Relationships between intrinsic population growth rate, carrying capacity and metabolism in microbial populations. The ISME Journal Pages 1–4.

Maurer, B. A. 1996. Relating human population growth to the loss of biodiversity. Biodiversity Letters 3:1–5.

367 McCann, K., Hastings, A., and Huxel, G. R. 1998. Weak trophic interactions and the balance
368   of nature. Nature 395:794–798.

369 Medeiros, L. P., Boege, K., del Val, E., Zaldivar-Riverón, A., and Saavedra, S. 2021a. Observed
370   ecological communities are formed by species combinations that are among the most likely
371   to persist under changing environments. The American Naturalist 197:E17–E29.

372 Medeiros, L. P., Song, C., and Serguei, S. 2021b. Merging dynamical and structural indicators
373   of resilience. J. of Animal Ecology 90:2027–2040.

374 Michaelian, K. 2005. Thermodynamic stability of ecosystems. Journal of Theoretical Biology
375   237:323 – 335.

376 Odum, E. P. and Barrett, G. W., 2005. Fundamentals of Ecology. Thomson, Brooks-Cole, Fifth
377   Edition.

378 Parain, E. C., Rohr, R. P., Gray, S. M., and Bersier, L.-F. 2019. Increased temperature disrupts
379   the biodiversity–ecosystem functioning relationship. The American Naturalist 193:227–239.

380 Pawar, S., Dell, A. I., and Savage, V. M. 2012. Dimensionality of consumer search space drives
381   trophic interaction strengths. Nature 486:485–489.

382 Rohr, R. P., Saavedra, S., Peralta, G., Frost, C. M., Bersier, L.-F., Bascompte, J., and
383   Tylianakis, J. M. 2016. Persist or produce: a community trade-off tuned by species evenness.
384   Am. Nat. 188:411–422.

385 Saavedra, S. 2024. The feasibility principle in community ecology. EcoEvoRxiv
386   10.32942/X2X05W.

387 Saavedra, S., Medeiros, L. P., and AlAdwani, M. 2020. Structural forecasting of species persis-
388   tence under changing environments. Ecology Letters 23:1511–1521.

389 Saavedra, S., Rohr, R. P., Bascompte, J., Godoy, O., Kraft, N. J., and Levine, J. M. 2017.
390   A structural approach for understanding multispecies coexistence. Ecological Monographs
391   87:470–486.

392 Saavedra, S., Rohr, R. P., Fortuna, M. A., Selva, N., and Bascompte, J. 2016. Seasonal
393   species interactions minimize the impact of species turnover on the likelihood of community
394   persistence. Ecology 97:865–873.

395 Savage, V. M., Gillooly, J. F., Brown, J. H., West, G. B., and Charnov, E. L. 2004. Effects of
396   body size and temperature on population growth. The American Naturalist 163:429–441.

18

Segura, A. M. and Perera, G. 2023. Metabolic constraints on the body size scaling of extreme population densities. Ecology Letts 26:919–928.

Shestopaloff, Y. K. 2024. Metabolic allometric scaling of multicellular organisms as a product of evolutionary development and optimization of food chains. Biophysical Reviews and Letters 19:67–119.

Song, C., Altermatt, F., Pearse, I., and Saavedra, S. 2018a. Structural changes within trophic levels are constrained by within-family assembly rules at lower trophic levels. Ecology Letters 21:1221–1228.

Song, C., Rohr, R. P., and Saavedra, S. 2018b. A guideline to study the feasibility domain of multi-trophic and changing ecological communities. J. of Theoretical Biology 450:30–36.

Song, C. and Saavedra, S. 2018. Will a small randomly-assembled community be feasible and stable? Ecology 99:743–751.

Tabi, A., Gilarranz, L. J., Wood, S. A., Dunne, J. A., and Saavedra, S. 2023. Protection promotes energetically efficient structures in marine communities. PLoS Computational Biology 19:e1011742.

Tabi, A., Pennekamp, F., Altermatt, F., Alther, R., Fronhofer, E. A., Horgan, K., Machler, E., Pontarp, M., Petchey, O. L., and Saavedra, S. 2020. Species multidimensional effects explain idiosyncratic responses of communities to environmental change. Nature Ecology & Evolution 4:1036–1043.

Täuber, U. C. 2011. Stochastic population oscillations in spatial predator-prey models. Journal of Physics: Conference Series 319:012019.

Vandermeer, J. H. 1970. The community matrix and the number of species in a community. The American Naturalist 104:73–83.

Vandermeer, J. H. and Goldberg, D. E., 2013. Population ecology: first principles. Princeton University Press.

Vasseur, D. A. and McCann, K. S. 2005. A mechanistic approach for modeling temperature-dependent consumer-resource dynamics. Am. Nat. 166:184–198.

Vellend, M., 2016. The theory of ecological communities. Princeton University Press, NJ.

West, G. B., Brown, J. H., and Enquist, B. J. 1997. A general model for the origin of allometric scaling laws in biology. Science 276:122–126.

427 Yeakel, J. D., Kempes, C. P., and Redner, S. 2018. Dynamics of starvation and recovery predict

428   extinction risk and both Damuth's law and Cope's rule. Nature Communications 9:657.

429 Yodzis, P. and Innes, S. 1992. Body size and consumer-resource dynamics. The American

430   Naturalist 132:1151–1175.

431 Zaoli, S., Giometto, A., Maritan, A., and Rinaldo, A. 2017. Covariations in ecological scaling

432   laws fostered by community dynamics. Proceedings of the National Academy of Sciences

433   114:10672–10677.

Appendix S1

Integrating metabolic scaling and coexistence theories

The estimation of time-independent, area-independent, competitive interactions a_{ij} is derived by translating classic consumer-resource dynamics into Lotka-Volterra competition dynamics following Vandermeer and Goldberg (2013).

Let us assume that there are two self-replicating resources:

$$\begin{cases} \dfrac{\mathrm{d}R_1}{\mathrm{d}t} = r_{\mathrm{rsc}_1} R_1 \left[\left(\dfrac{k_1 - R_1}{k_1} \right) - c_{11} N_1 - c_{12} N_2 \right], \\[2ex] \dfrac{\mathrm{d}R_2}{\mathrm{d}t} = r_{\mathrm{rsc}_2} R_2 \left[\left(\dfrac{k_2 - R_2}{k_2} \right) - c_{21} N_1 - c_{22} N_2 \right], \end{cases} \tag{1}$$

where R_i is the biomass density of the resource i (dimensions [mass]·[area]$^{-1}$), r_{rsc_i} is the intrinsic rate of increase of resource i (dimension [time]$^{-1}$), k_i is the carrying capacity of biomass density of the resource i (dimensions [mass]·[area]$^{-1}$), c_{ij} is the time-independent rate at which the resource i is consumed by the jth consumer across unit area (dimensions [mass$_j$]$^{-1}$·[area]), and N_i is the population biomass density of the ith consumer (dimensions [mass]·[area]$^{-1}$).

Then, considering two consumers, we can write the consumer equations:

$$\begin{cases} \dfrac{\mathrm{d}N_1}{\mathrm{d}t} = N_1 \left(b_{11} R_1 + b_{12} R_2 - d_1 \right), \\[2ex] \dfrac{\mathrm{d}N_2}{\mathrm{d}t} = N_2 \left(b_{21} R_1 + b_{22} R_2 - d_2 \right), \end{cases} \tag{2}$$

where b_{ij} is the relative conversion of a unit of resource j by consumer i across unit area per time (dimensions [mass$_j$]$^{-1} \cdot$ [time]$^{-1}$·[area]), and d_i is the death rate of the ith consumer (dimension [time]$^{-1}$). Note that b_{ij} is different from mass transformation efficiency.

Assuming that the dynamics of the resources occur significantly faster than those of the consumers (MacArthur and Levins, 1967), we can equate the derivatives of Eqs. (1) to zero and solve for the equilibrium values R_1^* and R_2^* of the two resources:

$$\begin{aligned} R_1^* &= k_1(1 - c_{11} N_1 - c_{12} N_2), \\ R_2^* &= k_2(1 - c_{21} N_1 - c_{22} N_2). \end{aligned} \tag{3}$$

1

Then, we can substitute R_1 and R_2 in Eqs. (2) by R_1^* and R_2^*, respectively. That is,

$$\begin{cases} \dfrac{\mathrm{d}N_1}{\mathrm{d}t} = N_1 \left[b_{11}k_1(1 - c_{11}N_1 - c_{12}N_2) + b_{12}k_2(1 - c_{21}N_1 - c_{22}N_2) - d_1 \right], \\ \dfrac{\mathrm{d}N_2}{\mathrm{d}t} = N_2 \left[b_{21}k_1(1 - c_{11}N_1 - c_{12}N_2) + b_{22}k_2(1 - c_{21}N_1 - c_{22}N_2) - d_2 \right], \end{cases} \tag{4}$$

which can also be written as

$$\begin{cases} \dfrac{\mathrm{d}N_1}{\mathrm{d}t} = N_1 \left[b_{11}k_1 + b_{12}k_2 - d_1 - (b_{11}k_1c_{11} + b_{12}k_2c_{21})N_1 - (b_{11}k_1c_{12} + b_{12}k_2c_{22})N_2 \right], \\ \dfrac{\mathrm{d}N_2}{\mathrm{d}t} = N_2 \left[b_{21}k_1 + b_{22}k_2 - d_2 - (b_{21}k_1c_{11} + b_{22}k_2c_{21})N_1 - (b_{21}k_1c_{12} + b_{22}k_2c_{22})N_2 \right]. \end{cases} \tag{5}$$

Multiplying and dividing the two equations in Eqs. (5) by

$$b_{11}k_1 + b_{12}k_2 - d_1,$$
$$b_{21}k_1 + b_{22}k_2 - d_2, \tag{6}$$

respectively, we obtain

$$\begin{cases} \dfrac{\mathrm{d}N_1}{\mathrm{d}t} = (b_{11}k_1 + b_{12}k_2 - d_1)N_1 \left[\dfrac{b_{11}k_1 + b_{12}k_2 - d_1 - (b_{11}k_1c_{11} + b_{12}k_2c_{21})N_1 - (b_{11}k_1c_{12} + b_{12}k_2c_{22})N_2}{b_{11}k_1 + b_{12}k_2 - d_1} \right], \\ \dfrac{\mathrm{d}N_2}{\mathrm{d}t} = (b_{21}k_1 + b_{22}k_2 - d_2)N_2 \left[\dfrac{b_{21}k_1 + b_{22}k_2 - d_2 - (b_{21}k_1c_{11} + b_{22}k_2c_{21})N_1 - (b_{21}k_1c_{12} + b_{22}k_2c_{22})N_2}{b_{21}k_1 + b_{22}k_2 - d_2} \right]. \end{cases} \tag{7}$$

Again, dividing both the numerator and denominator of the fractions on the right sides of the two equations in Eqs. (7) by

$$b_{11}k_1c_{11} + b_{12}k_2c_{21},$$
$$b_{21}k_1c_{12} + b_{22}k_2c_{22}, \tag{8}$$

respectively, gives us

$$\begin{cases} \dfrac{\mathrm{d}N_1}{\mathrm{d}t} = (b_{11}k_1 + b_{12}k_2 - d_1)N_1 \left[\dfrac{\frac{b_{11}k_1 + b_{12}k_2 - d_1}{b_{11}k_1c_{11} + b_{12}k_2c_{21}} - N_1 - \frac{b_{11}k_1c_{12} + b_{12}k_2c_{22}}{b_{11}k_1c_{11} + b_{12}k_2c_{21}}N_2}{\frac{b_{11}k_1 + b_{12}k_2 - d_1}{b_{11}k_1c_{11} + b_{12}k_2c_{21}}} \right], \\ \dfrac{\mathrm{d}N_2}{\mathrm{d}t} = (b_{21}k_1 + b_{22}k_2 - d_2)N_2 \left[\dfrac{\frac{b_{21}k_1 + b_{22}k_2 - d_2}{b_{21}k_1c_{12} + b_{22}k_2c_{22}} - \frac{b_{21}k_1c_{11} + b_{22}k_2c_{21}}{b_{21}k_1c_{12} + b_{22}k_2c_{22}}N_1 - N_2}{\frac{b_{21}k_1 + b_{22}k_2 - d_2}{b_{21}k_1c_{12} + b_{22}k_2c_{22}}} \right]. \end{cases} \tag{9}$$

Essentially, Eqs. (9) are the Lotka-Volterra competition dynamics, which can be easily recog-

nized if we make the following substitutions

$$
\begin{aligned}
r_1 &\triangleq b_{11}k_1 + b_{12}k_2 - d_1, \\
r_2 &\triangleq b_{21}k_1 + b_{22}k_2 - d_2, \\
K_1 &\triangleq \frac{b_{11}k_1 + b_{12}k_2 - d_1}{b_{11}k_1c_{11} + b_{12}k_2c_{21}}, \\
K_2 &\triangleq \frac{b_{21}k_1 + b_{22}k_2 - d_2}{b_{21}k_1c_{12} + b_{22}k_2c_{22}},
\end{aligned}
\tag{10}
$$

and

$$
\begin{aligned}
a_{12} &\triangleq \frac{b_{11}k_1c_{12} + b_{12}k_2c_{22}}{b_{11}k_1c_{11} + b_{12}k_2c_{21}} = \frac{C_2(b_{11}k_1n_{12} + b_{12}k_2n_{22})}{C_1(b_{11}k_1n_{11} + b_{12}k_2n_{21})} = \frac{C_2}{C_1} \cdot \text{normalization constant}, \\
a_{21} &\triangleq \frac{b_{21}k_1c_{11} + b_{22}k_2c_{21}}{b_{21}k_1c_{12} + b_{22}k_2c_{22}} = \frac{C_1(b_{21}k_1n_{11} + b_{22}k_2n_{21})}{C_2(b_{21}k_1n_{12} + b_{22}k_2n_{22})} = \frac{C_1}{C_2} \cdot \text{normalization constant},
\end{aligned}
\tag{11}
$$

where r_i is the rate of natural increase in isolation of consumer i (dimension $[\text{time}]^{-1}$), K_i is the carry capacity of consumer i biomass density in the absence of all competitors (dimensions $[\text{mass}]\cdot[\text{time}]^{-1}$), and a_{ij} is the time-independent, area-independent, competition coefficient measuring the competitive effect of consumer j on consumer i (dimensions $[\text{mass}_i]\cdot[\text{mass}_j]^{-1}$). Specifically, C_j is the time-independent average rate at which consumer j consumes resources across unit area (dimensions $[\text{mass}]^{-1}\cdot[\text{area}]$). Furthermore, it is typically observed that the relative conversion b_{ij} of a unit of resource j by consumer i and the carrying capacity k_j of resource j have limited variations for a given consumer i across different resources j and can be assumed constant for the sake of model simplification (Brown et al., 2004). Therefore, as indicated by Eq. (11), it is important to note that the competition coefficient a_{ij} is proportional to the ratio of consumption rates C between consumer j and consumer i. Formally, we can represent it as

$$
a_{ij} = a_0' \left(\frac{C_j}{C_i} \right),
\tag{12}
$$

where a_0' is an *effective* parameter (dimensionless) representing the overall effect of intrinsic properties, such as consumers' conversion rates (Parain et al., 2019).

To further estimate the time-independent average rate C_i at which consumer i consumes resources, we can simplify the previous scenario by considering a streamlined framework that involves only one consumer (also predator, either consumer j or consumer i) and one resource (also prey). Specifically, if the resource is self-replicating, then the resource equation with a logistic growth is

$$
\frac{\mathrm{d}R}{\mathrm{d}t} = rR\left[\left(\frac{k-R}{k} \right) - cN \right],
\tag{13}
$$

where R is the biomass density of the resource (dimensions [mass]·[area]$^{-1}$), r is its per capita rate of increase (dimension [time]$^{-1}$), k is the carrying capacity of biomass density of the resource (dimensions [mass]·[area]$^{-1}$), c is the time-independent rate at which the resource is consumed by the consumer across unit area (dimensions [area]·[mass]$^{-1}$), and N is the biomass density of the consumer (dimensions [mass]·[area]$^{-1}$).

Then, we can write the consumer equation as

$$\frac{\mathrm{d}N}{\mathrm{d}t} = (bR - d)N, \tag{14}$$

where b is the area-independent predation rate (dimensions [mass$_R$]$^{-1}$·[time]$^{-1}$) and d is the death rate of the consumer (dimension [time]$^{-1}$).

Assuming again that the resource dynamics are very fast compared to the consumer dynamics (MacArthur and Levins, 1967), we can solve the equilibrium value of R:

$$R^* = k(1 - CN), \tag{15}$$

and then substitute R^* in place of R in the consumer equation Eq. (14). We obtain

$$\frac{\mathrm{d}N}{\mathrm{d}t} = [bk(1 - CN) - d]N, \tag{16}$$

which can also be written as

$$\frac{\mathrm{d}N}{\mathrm{d}t} = N(bk - d - bkCN). \tag{17}$$

Multiplying and dividing Eq. (17) by $(bk - m)$ gives us

$$\frac{\mathrm{d}N}{\mathrm{d}t} = (bk - d)N\left(\frac{bk - d - bkCN}{bk - d}\right). \tag{18}$$

Next, dividing both the numerator and the denominator of the fraction on the right side of the Eq. (18) by bkC, we have

$$\frac{\mathrm{d}N}{\mathrm{d}t} = (bk - m)N\left(\frac{\frac{bk-d}{bkC} - N}{\frac{bk-d}{bkC}}\right). \tag{19}$$

If we denote

$$
\begin{aligned}
r &\triangleq bk - d, \\
K &\triangleq \frac{bk - d}{bkC},
\end{aligned}
\tag{20}
$$

then Eq. (19) can be written as the classic population model with logistic growth:

$$\frac{\mathrm{d}N}{\mathrm{d}t} = rN \left(\frac{K - N}{K} \right), \tag{21}$$

where again r is the rate of natural increase in isolation of the consumer (dimension $[\text{time}]^{-1}$) and K is the carrying capacity of the consumer without competitors (dimensions $[\text{mass}]\cdot[\text{area}]^{-1}$).

Importantly, Eqs. (20) indicate that the time-independent consumption rate C increases monotonically with the intrinsic growth rate r (Deng et al., 2024). Formally, by substituting the expression for bk as $(r + d)$ from the first equation into the second equation, we obtain

$$C = \frac{1}{K \left(1 + \frac{d}{r} \right)}. \tag{22}$$

The time-independent consumption rate C (dimensions $[\text{area}]\cdot[\text{mass}]^{-1}$) exhibits a monotonically decreasing behavior with respect to the carrying capacity K (dimensions $[\text{mass}]\cdot[\text{area}]^{-1}$). Note that the relationship between carrying capacity K and intrinsic growth rate r appears to be complex and context-dependent (Marshall et al., 2023). Therefore, instead of establishing relationships between r and K, our primary focus lies on K due to its role in the feasibility of Lotka-Volterra competition dynamics. However, the focus can be shifted to r (Deng et al., 2024).

Following metabolic scaling theory (Eqs. 2-3 in main text), one can write the time-independent average consumption rate of population i (Eq. 35) as a function of body size (M_i). Note that mortality rate (d_i) is the reciprocal of generation time (G_i) and proportional to growth rate (r_i). For a fixed thermal domain and response, we can replace the parameters in Eq. 37 with the following equivalences: $r_i = r_0 \cdot M_i^{-1/4}$, $d_i = d_0 \cdot M_i^{-1/4}$, $K_i = K_0 \cdot M_i^{-3/4} \cdot M_i = K_0 \cdot M_i^{1/4}$, where r_0, d_0, and K_0 are normalization constants. Thus, Eq. (35) can be expressed as:

$$C_i = a_0'' \cdot M_i^{-1/4}. \tag{23}$$

Eventually, by combining Eq. (12) with Eq. (36), we can derive an estimation of time-independent, area-independent, competitive interaction strength a_{ij} for a fixed thermal domain and response as:

$$a_{ij} = a_0 \cdot (M_j/M_i)^{-1/4}, \tag{24}$$

where a_0', a_0'', and a_0 are normalization constants. Based on this estimation, we can generate

5

the competition matrix $\mathbf{A}$ for the Lotka-Volterra competition dynamics in Eq. (4) in main text.

Under $a_{ij} = a_0 \cdot (M_j/M_i)^{-1/4}$ (Eq. 39), Figure 2 (main text) shows that if the carrying capacities of biomass densities are defined as $K_i = K_0 \cdot M_i^{-3/4} \cdot M_i = K_0 \cdot M_i^{1/4}$, then they are the closest to the centroid of the feasibility domain. However, these carrying capacities $\boldsymbol{K}$ are expected to become exactly the centroid only under a specific value of a_0. For example, following Eq. 39 and for two competing species, the maximum and minimum feasible carrying capacities for species 2 (corresponding to the spanning vectors of the feasibility domain in Fig. 1) can be defined as $K_{2\text{max}} = (a_{22}/a_{12})K_1$ and $K_{2\text{min}} = (a_{21}/a_{11})K_1$, where $K_1 = K_0 \cdot M_1^{1/4}$ is the carrying capacity of biomass density of species 1 per metabolic scaling theory. Then, following Eq. 9, the carrying capacity for species 2 that belongs to the centroid of the feasibility domain becomes:

$$K_{2\text{c}} = \frac{1}{2}(K_{2\text{max}} + K_{2\text{min}}). \tag{25}$$

Note that in the centroid the distance beteween K_{2c} and K_1 should be the absolute minimum, i.e., $K_{2c}/K_1 = 1$. Thus, diving Eq. 40 by the carrying capacities of biomass density of species 1 (K_1) and rearranging it yields:

$$(M_2/M_1)^{-1/4} = \frac{1}{2} \cdot \frac{1 + a_0^2}{a_0} \cdot (M_2/M_1)^{-1/4}. \tag{26}$$

This implies that the equality is satisfied if and only if the factor $\frac{1+a_0^2}{2a_0} = 1$. Since a_0 also affects the dynamical stability of the community, future work can investigate the possible trade-offs between stability and feasibility under this framework. However, under numerical simulations, the larger the community, the closer this expression becomes the centroid of the feasibility domain.

The vector $K_i = K_0 \cdot M_i^{1/4}$ tends to get asymptotically closer to the centroid of the feasibility domain the larger the community (Fig S1). Specifically, following Eq. 14 in main text, we generated an ensemble of 10^4 competition matrices $\mathbf{A}$ characterizing the time-independent, area-independent, competitive effects (a_{ij}) between $10, 20, 50, 100, 200, 500$, and 1000 populations. Each matrix was formed by drawing M_i values independently from a lognormal distribution $LN(0, 2)$. These distributions can change without affecting the qualitative results. Following previous work (Bunin, 2017, Dougoud et al., 2018), we set the effective parameter of competitive effects to $a_0 = |\mathcal{S}|^{-1/2}$ for $i \neq j$, otherwise $a_0 = 1$. This assumption follows the rationale that empirical interactions tend to be weak, stabilizing communities (Gellner et al., 2023, McCann et al., 1998). The greater the value of a_0, the greater the overall competition, and the smaller

6

the range of the feasibility domain. Then, we calculated the average distance between $\boldsymbol{K_c}(\mathbf{A})$ and $\boldsymbol{K}$ as (Medeiros et al., 2021b, Saavedra et al., 2017)

$$d(\mathbf{A}, \boldsymbol{K}) = \arccos(\boldsymbol{K} \cdot \boldsymbol{K_c}(\mathbf{A}) \cdot ||\boldsymbol{K}||^{-1} \cdot ||\boldsymbol{K_c}(\mathbf{A})||^{-1}) \in [0, 90]. \qquad (27)$$

Note that the normalization constant K_0 of carrying capacities of biomass densities does not affect this distance and can be omitted from the equation (Rohr et al., 2016). This numerical analysis reveal that the large the number of populations, the smaller the distance to the centroid.
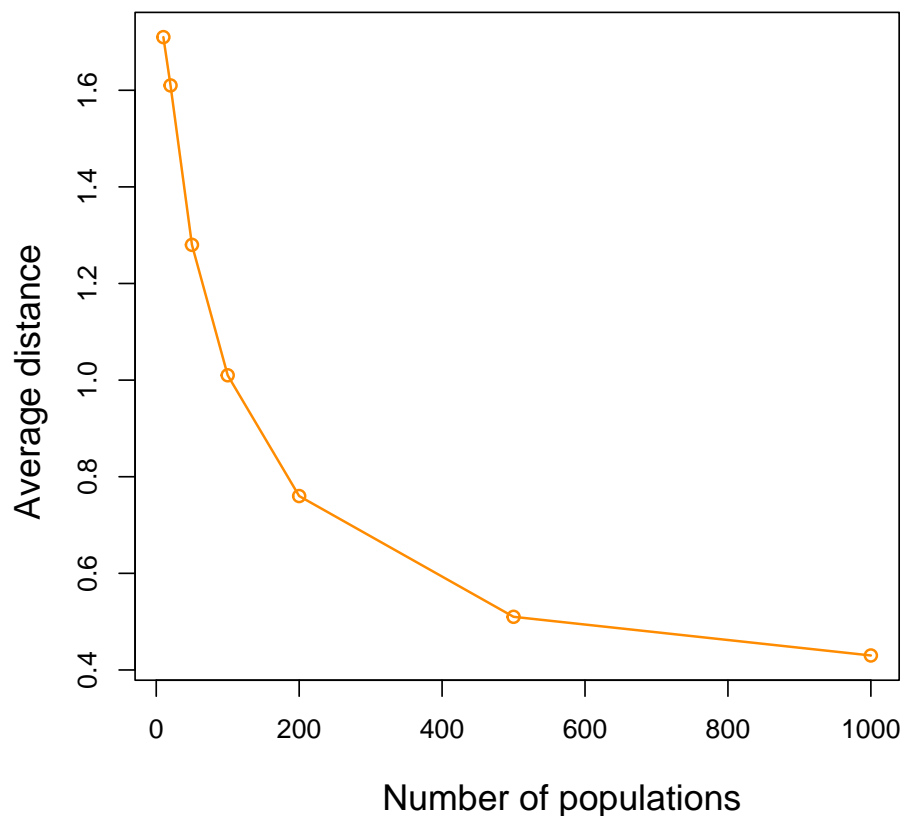

Figure 1: **Distance to the centroid for large communities**. For an ensemble of 10^4 generated competition matrices with different number of populations, we show the average distance between the vector $K_i = K_0 \cdot M_i^{1/4}$ and the centroid of the feasibility domain. This numerical analysis reveal that the large the number of populations, the smaller the distance to the centroid.